

J Neurol (2013) 260:1601–1610  
DOI 10.1007/s00415-013-6841-2

ORIGINAL COMMUNICATION

# Widespread grey matter changes and hemodynamic correlates to interictal epileptiform discharges in pharmacoresistant mesial temporal epilepsy

Roland Wiest · Lea Estermann · Olivier Scheidegger ·  
Christian Rummel · Kay Jann · Margitta Seeck ·  
Kaspar Schindler · Martinus Hauf

Received: 25 July 2012/Revised: 9 January 2013/Accepted: 11 January 2013/Published online: 26 January 2013  
© Springer-Verlag Berlin Heidelberg 2013

**Abstract** Focal onset epilepsies most often occur in the temporal lobes. To improve diagnosis and therapy of patients suffering from pharmacoresistant temporal lobe epilepsy it is highly important to better understand the underlying functional and structural networks. In mesial temporal lobe epilepsy (MTLE) widespread functional networks are involved in seizure generation and propagation. In this study we have analyzed the spatial distribution of hemodynamic correlates (HC) to interictal epileptiform discharges on simultaneous EEG/fMRI recordings and relative grey matter volume (rGMV) reductions in 10 patients with MTLE. HC occurred beyond the seizure onset zone in the hippocampus, in the ipsilateral insular/operculum, temporo-polar and lateral neocortex, cerebellum, along the central sulcus and bilaterally in the cingulate

gyrus. rGMV reductions were detected in the middle temporal gyrus, inferior temporal gyrus and uncus to the hippocampus, the insula, the posterior cingulate and the anterior lobe of the cerebellum. Overlaps between HC and decreased rGMV were detected along the mesolimbic network ipsilateral to the seizure onset zone. We conclude that interictal epileptic activity in MTLE induces widespread metabolic changes in functional networks involved in MTLE seizure activity. These functional networks are spatially overlapping with areas that show a reduction in relative grey matter volumes.

**Keywords** Mesial temporal lobe epilepsy · EEG/fMRI · Network analysis · Voxel based morphometry

R. Wiest (✉) · L. Estermann · O. Scheidegger · C. Rummel ·  
M. Hauf

Support Center of Advanced Neuroimaging (SCAN),  
University Institute of Diagnostic and Interventional  
Neuroradiology, Inselpital, University of Bern,  
3010 Bern, Switzerland  
e-mail: Roland.Wiest@insel.ch

K. Jann  
Department of Psychiatric Neurophysiology,  
University Hospital of Psychiatry, University of Bern,  
Bern, Switzerland

M. Seeck  
Epilepsy Unit, Department of Neurology,  
University of Geneva, Geneva, Switzerland

K. Schindler  
Epilepsy Unit, Department of Neurology,  
University of Bern, Bern, Switzerland

M. Hauf  
Bethesda Epilepsy Clinic, 3233 Tschugg, Switzerland

## Introduction

Specific cortical and subcortical networks are increasingly recognized as fundamental elements that contribute to the generation and spread of focal onset seizures throughout the human brain [2, 23, 24, 47]. These networks are represented either by structural modifications or by functional characteristics of electric activity in the human cortex. In mesial temporal lobe epilepsy (MTLE), such structural abnormalities extend widely beyond the seizure onset zone (SOZ) in the mesial temporal lobe. Structural alterations (i.e., volume loss and reduced synaptic density) have been identified in the insula, the parahippocampal and lingual gyrus, the frontal neocortex, the cingulate gyrus, and the thalamus [5, 7, 16, 42]. The extent of temporal and extra-temporal atrophy correlates well with duration and severity of epilepsy [8, 12]. Moreover, a correlation between distinct seizure semiology and topography of structural alterations has been reported [46]. Excitotoxic effects

during seizures and interictal epileptiform discharges may lead to neuronal loss [33, 48], but the underlying processes driving the progression of cortical changes are still not fully understood. Characteristic propagation patterns of epileptic activity recorded with intracranial EEG and ictal SPECT in MTLE have been identified resembling three major physiological neuronal networks: (1) the medial temporal/limbic network, (2) the superior parietal/medial frontal network and (3) the medial occipital/lateral temporal network [23, 49]. The reciprocal excitatory and inhibitory interconnections within the networks are essential for normal information processing, as those of language and memory [14, 54], but may also transmit abnormal signals in epileptic disorders [38].

In epilepsy, characterization of temporal network functions based on signal propagation is rigorous and most informative when analyzed by intracranial EEG. Spatial network distributions, however, may be more accurately detected by functional neuroimaging. Investigation of hemodynamic correlates (HC) linked to interictal epileptiform discharges (IEDs) by simultaneous EEG/fMRI is an increasingly recognized approach to studying spatial compositions of epileptic networks during seizure-free periods. EEG/fMRI studies have explored network properties of HC in temporal lobe epilepsy and HC in the temporal and extratemporal cortex have been reported [18, 32, 35]. However, the extent of metabolic changes and their role in the pathophysiology of seizure generation and spread remains unclear. Following studies dedicated to the identification of local abnormalities, we expect that studies of epileptic activity and its substrate will focus increasingly on large-scale network aspects. Here, we report the group analysis of simultaneous EEG/fMRI recordings in a series of MTLE patients in order to identify the relationship between HC and IEDs and structural alterations. We hypothesized that HC linked to IEDs reflect the large-scale topography of structurally altered brain areas and indicate core structures in MTLE networks.

## Methods

### Subjects

Ten right-handed patients from the local presurgical epilepsy programme who underwent EEG/fMRI were retrospectively selected from our database. Mean age of the patients was  $40.1 \pm 15.7$  years (range 20–68 years, 3 females). Inclusion criteria were (a) mesial temporal lobe epilepsy, (b) interictal discharges during the EEG/fMRI recordings and presence of BOLD correlates in the SOZ [29]. All patients had a history of partial-complex seizures (mean duration 25.1 years, range 2–47 years). Structural

neuroimaging was performed by high-resolution MRI at 3T using a dedicated epilepsy protocol [27]. In addition, 10 right-handed gender and age matched healthy controls were recruited on a voluntary basis (mean age  $40.7 \pm 13.2$  years, range 23–66 years, seven males and three females). All study participants gave written informed consent. The study was approved by the institutional ethics committee in accordance with the Declaration of Helsinki. Individual data of patients 1–4 and 6–9 have been published previously in a case series to evaluating the localization value of the SOZ by EEG/fMRI recordings [25].

### MRI setup and acquisition

MRI was performed on a 3T Siemens Magnetom Trio TIM system (Siemens AG, Erlangen, Germany). High-resolution three-dimensional (3D) volume images were obtained using a multiplanar rapid gradient echo sequence (MP-RAGE, 176 sagittal slices, isovoxel resolution = 1.0 mm, FOV  $256 \times 256$  mm, matrix size =  $256 \times 256$ , TR/TE/TI = 1,950/2.15/900 ms). Functional MRI was performed with a multi-slice single-shot T2\*-weighted echo planar imaging sequence (32 slices, slice thickness = 3 mm, gap thickness = 0.75 mm, TR/TE = 1,980/30 ms; matrix size  $64 \times 64$  mm; FoV  $192 \times 192$  mm; flip angle:  $90^\circ$ ) with a total of 460 volumes.

### Voxel-based morphometry (VBM) analysis

Every scan was checked for image artifacts and gross anatomical abnormalities. The SOZ of three patients (Patient 5, 6 and 10) was determined in the left mesial temporal lobe and the images were flipped accordingly in advance of further processing. Postprocessing, and data analysis was performed with SPM 5, using the VBM 5.1 toolbox (<http://dbm.neuro.uni-jena.de>) running with Matlab 7.1 (The MathWorks, Natick, MA) [37]. To identify effects of relative volumes corrected for different brain sizes and shapes, a modulation step correcting for non-linear warping was performed. Processing for VBM included unified segmentation with hidden Markov random field on the estimated tissue maps ( $3 \times 3 \times 3$  voxel) [40]. Images were processed using International Consortium for Brain Mapping template (ICBM) tissue priors, modulated normalization, bias correction and affine registration. Smoothing was performed at a 8-mm full-width at half-maximum Gaussian kernel resulting in final tissue maps of grey matter (GM), white matter (WM) and cerebrospinal fluid (CSF). Age and total intracranial volume (TIV) were classified as nuisance covariates in the comparisons of GM volumes between MTLE and normal healthy controls. Analysis was restricted to the grey matter maps in order to

identify the core areas of relative GM volume reduction between the patients and healthy controls [41]. Morphologic differences were estimated with two-sample student  $t$  tests. In VBM analysis, a map of the  $t$  statistic was generated by assigning each voxel to the test value, where inferences about rGMV differences were made at a combined voxel level of  $t = 3.1$  (uncorrected) and a cluster size extent threshold level of 1,600 voxels (1,600 mm<sup>3</sup>) resulting in a threshold corrected for multiple comparison of  $p < 0.05$ .

#### EEG/fMRI setup, recording, preprocessing, and intrasubject data analysis procedures

Setup, recording, preprocessing, and data analysis of the individual EEG and fMRI data were performed as described in Jann et al. [29]. The EEGs recorded outside and inside the MR scanner were concatenated and decomposed into independent components (IC) applying an extended infomax independent component analysis (ICA) algorithm [15]. Volumes with artifacts in the corresponding EEG epoch (e.g., motion, residual MR-artifacts) were excluded from analysis. The resulting ICs were visually inspected by two experienced electroencephalographers (RW, MH) taking into account their temporal dynamics (i.e., the epileptiform activity and the loadings of the selected IC occur at the same timepoints) and the scalp distributions of IEDs in the original EEG and the specific IC scalp map (weighting of IC-factor onto the single electrodes). The IC best representing the interictal epileptiform activity was then selected by consent [26], convolved with a standard double gamma hemodynamic response function (HRF) [22] and used as predictor for the fMRI BOLD signal in the correlation estimation. Preprocessing of the functional MR-dataset consisted of slice-scan time correction, removal of low-frequency drifts, 3D motion detection and correction, and spatial smoothing with a Gaussian Kernel of 8 mm FWHM. Co-registration of the 2D functional to the 3D structural images was performed using the scanner's slice position parameters of the T2\*-weighted measurements and the T1-weighted anatomical measurements. Individual anatomical and functional data sets were co-registered and normalized to the Talairach space and masked to grey matter (BrainVoyagerQX 1.10.2 (Brain Innovation, Maastricht, The Netherlands)). Correlation estimation between the IC-based predictor of the IEDs and the BOLD signal were computed using a General linear model (cf. Fig. 1).

#### Group analysis

The rate of IEDs on the surface EEG ranged between 1 and 2.5/min in all patients during recordings and facilitated a balanced design for the group analysis [20]. The spatially

normalized maps from the correlation estimation of the HC to the IEDs corresponding to left MTLE patients were right-left flipped (patient 5, 6, 10), such that the hemisphere ipsilateral to the SOZ zone is the right hemisphere in the stereotactic space. A single t-contrast image was generated per subject from the single-subject level and the map used to inform a second level (group effect) analysis to test for any common pattern. HCs at the group level were evaluated using a one sample  $t$  test. HC clusters were considered significant at an uncorrected statistical height threshold of  $t \geq 2.6$  as applied in two recent group analyses of EEG/fMRI recordings [18, 32]. Correction for multiple comparisons at  $p < 0.05$  was done by spatial extent thresholding with a cluster sizes of 38 functional voxels (1,026 mm<sup>3</sup>) calculated according to Forman et al. [19] using the spatial extent thresholding plug-in of BrainVoyager. Overlays of HC and rGMV were computed in MNI space and quantified using the dice similarity coefficient (DSC) [31].

## Results

Clinical data, EEG and structural imaging findings have been summarized in Table 1. All patients enrolled in the study presented with lesional MTLE proven by high-resolution MRI. Nine patients had a hippocampal sclerosis, seven patients within the right hippocampus, two within the left. One patient had a midtemporal cortical dysplasia of the left amygdala and hippocampus. Mesiotemporal seizure onset was proven by ictal semiology, video-telemetry and the presence of a structural lesion in all patients. Eight of 10 patients underwent epilepsy surgery (selective anterior amygdalo-hippocampectomy in seven, anterior temporal lobectomy in one). Seven patients were seizure-free (Engel class Ia) after surgery; one patient (patient 7) had rare disabling seizures classified as Engel class II. Mean follow-up after surgery was 39 months (range 22–64 months).

#### HC correlated with interictal epileptic activity

Spatial extent and topography of the group-wide HC are displayed in Table 2 and in Fig. 2. The largest BOLD clusters were detected along the insula (MNI coordinates, 41; -12, 2) and the fusiform gyrus (30, -39, -23), the superior temporal gyrus (56, -6, -6) and anterior limbic lobe (37, -23, 26) including the hippocampus, insula and subcortical nuclei ipsilateral to the SOZ. The most significant BOLD response within the group was detected in the fusiform gyrus ipsilateral to the SOZ (30, -39, -23). Bilateral HC were detected in the anterior cingulate gyrus (8, 15, 22). In the contralateral hemisphere, activations were detected in the insula (-41, -12, 2) and superior

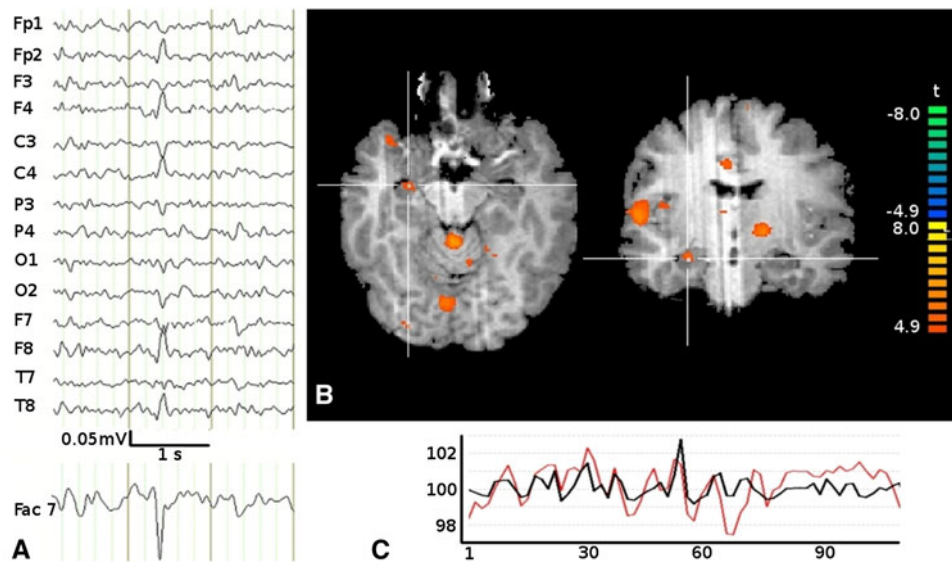


**Fig. 1** Right mesial temporal lobe epilepsy and right hippocampal sclerosis (patient 2). **a** Scalp EEG (average reference montage) and IC-factor coding for the interictal discharges with a right temporal maximum. **b** Positive BOLD correlates in the right mesial temporal lobe (crosshair), temporal pole, insula, middle cingulate gyrus,

cerebellum and left basal ganglia. **c** BOLD time course in the SOZ (hippocampus), as percentage of signal change, x-axis: no. of volumes, (red). Time course of the IC-factor derived from the EEG data after convolution with the hemodynamic response function representing the epileptic activity (black)

temporal gyrus ( $-50, 0, 1$ ), occipital lobe ( $-24, -73, 7$ ) and posterior cingulate gyrus ( $-10, -16, 35$ ). No HC was detected in the contralateral mesiotemporal lobe, in the corrected and uncorrected data. All clusters showed a positive BOLD correlate, whereas no deactivations were observed on the group level.

#### Brain areas with structural abnormalities and hemodynamic correlates to IEDs

In MTLE patients compared to gender and age matched healthy controls, there was a significant reduction of rGMV ipsilateral to the SOZ in the middle temporal gyrus ( $47, 6, -38$ ), inferior temporal gyrus ( $48, -13, -31$ ) and uncus to the hippocampus ( $25, 0, -40$ ), the insula ( $34, 12, -8$ ), the posterior cingulate ( $14, -49, 23$ ) and the anterior lobe of the cerebellum ( $13, -46, -31$ ). A spatial overlap between rGMV reductions and HC was detected ipsilateral to the SOZ along the mesial temporal/limbic network including the hippocampus ( $26, -3, -21$ ), temporal pole ( $46, 6, -33$ ), superior temporal gyrus ( $52, -6, -8$ ) and the posterior insula ( $37, -4, -6$ ). Within the posterior cingulate gyrus, the lingual gyrus rGMV reductions were within the same sublobar regions as the HCs. No rGMV were found within the contralateral hemisphere along brain areas with responses to IEDs (the anterior cingulate gyrus insula and superior temporal gyrus, occipital lobe and posterior cingulate gyrus). The set agreement (DCS) between the functional and the structural clusters was 6.5 % on the whole brain level. On the single cluster level, the spatial

overlaps were restricted to the hemisphere that encompassed the SOZ. Overlaps were detected between four out of 10 functional clusters and three out of five structural clusters with DSC varying between 0.5 and 33.1 %. The distribution of the brain regions with decreased rGMV are summarized in Table 3 and Fig. 3 the overlap of functional and anatomical changes in Table 4.

#### Discussion

Generation and spread of focal onset epileptic seizures involves a large network of brain areas that extend beyond the SOZ. The aim of this study was to investigate spatial patterns of HCs associated with interictal epileptic activity in relation to cortical rGMV alterations in a group of lesional MTLE patients. There are two key findings: (1) HC to IEDs beyond the SOZ are detected in brain areas along cortical networks that are expected to be involved based on clinical seizure semiology (the medial temporal/limbic network, the superior parietal/frontal network and the medial occipital/lateral temporal network) and (2) rGMV reductions are found within these networks in the mesiotemporal lobe, the temporal neocortex, the insula and the posterior cingulate cortex overlapping with hemodynamic changes. To our knowledge, this is the first study that investigated rGMV and HC associated with interictal epileptic activity within the same cohort of lesional MTLE patients.

Recent studies on interictal EEG/fMRI recordings have demonstrated that multifocal HC time-locked to IEDs

**Table 1** Clinical data, EEG and structural imaging findings of 10 patients with MTL

Patient no.	Age/sex	Epilepsy syndrome	Age of onset	Duration	Seizure frequency	sMRI	Semiology	Phase I (ictal videotelemetry, surface EEG)	Phase II invasive EEG	Operation/Date	Outcome: Engel Class
1	49/ M	MTLE R	11	38	4/month	HS R	Vocalisations, head turning to R; bimanual automatism		Surface + foramen ovale electrodes seizure onsets right mesiotemporal	sAHE R 03/07	I
2	31/ F	MTLE R	1	30	8/month	HS R	Head version to left, Fig. 4 sign with left tonic posturing	EEG consistent with right mesiotemporal seizure onsets		sAHE R 01/09	I
3	53/ F	MTLE R	4	49	2/month	HS R	Epigastric aura, vocalisations, oromandibular automatism, head turning to R, postictal cuffing	EEG consistent with right mesiotemporal seizure onsets		sAHE R 04/08	I
4	48/ M	MTLE R	10	38	2/month	HS R	Epigastric aura, oromandibular automatism, SG	EEG consistent with right mesiotemporal seizure onsets			
5	20/ F	MTLE L	16	4	NA	Hippocampal FCD L	Epigastric aura, SG	EEG consistent with left mesiotemporal seizure onsets			
6	31/ F	MTLE L	3	28	18/month	HS L	Epigastric aura, head turning to R, bimanual and perioral automatism		Surface + foramen ovale: seizure onsets left mesiotemporal	sAHE 8/10	I
7	68/ F	MTLE R	57	11	0.5/month	HS R	Nausea, oromandibular automatism	EEG consistent with right mesiotemporal seizure onsets		sAHE R 03/08	II
8	54/ F	MTLE R	52	2	1/month	HS R	Strange feeling, oromandibular automatism and bibrachial automatism		Surface + foramen ovale electrodes: seizure onsets left mesiotemporal	sAHE R 12/09	I
9	36/ F	MTLE R	5	31	10/month	HS R	Behavioural arrest, manual automatism right, dystonic posturing left arm	EEG consistent with right mesiotemporal seizure onset		sAHE R 9/2010	I
10	22/ F	MTLE L	5	15	NA	HS L	Manual automatism left, head-turning to the left, yawning		EEG with strip and depth electrodes: temporopolar to temporo-mesiotemporal left	Anterior temporal lobectomy 1/2010 L	I

M male, F female, R right, L left, HS hippocampus sclerosis, FCD focal cortical dysplasia, sAHE selective amygdalo-hippocampectomy

**Table 2** Clusters of significant HC to IEDs in patients with MTLE ( $p < 0.05$ , corrected)

Description		$p$ value uncorrected	MNI coordinates			Cluster size	$T$ (voxel level)
Global cluster maximum	Local maxima		$x$	$y$	$z$		
<b>Ipsilateral</b>							
Insula		0.0002	37	-23	26	1,658	5.35
	Hippocampus		20	-14	-25		
	Insula		37	-23	26		
	Globus pallidum		10	-6	1		
Superior temporal gyrus (temporo-polar)		0.00026	46	15	-28	3,666	5.80
Fusiformgyrus		0.00001	30	-39	-23	6,391	8.89
	Fusiform gyrus		30	-39	-23		
	Middle temporal gyrus		43	-60	5		
	Cerebellum		27	-62	-26		
Superior temporal gyrus		0.0005	56	-6	-6	3,411	5.36
Superior parietal lobule		0.001	30	-46	41	1,101	4.59
<b>Contralateral</b>							
Insula		0.00005	-41	-12	2	6,817	7.20
	Insula		-41	-12	2		
	Superior temporal gyrus		-50	0	1		
Occipital lobe		0.002	-24	-73	7	1,473	4.29
Inferior parietal lobule		0.0003	-56	-36	27	2,679	5.72
Posterior cingulate gyrus		0.00007	-10	-16	35	5,835	6.93
	Posterior cingulate gyrus		-10	-16	35		
	Postcentral gyrus		-19	-41	70		
<b>Bilateral</b>							
Anterior cingulate gyrus		0.0005	8	15	22	1,053	5.33

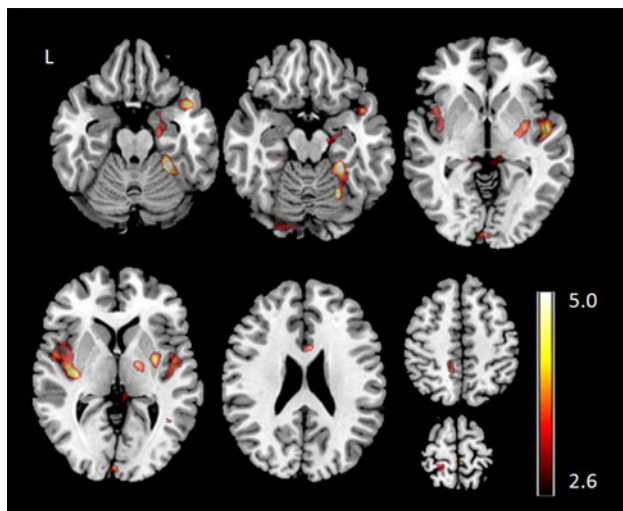


**Fig. 2** Group analysis of EEG/fMRI in 10 patients with MTLE (t-map at  $t > 2.6$  and additional cluster size threshold resulting in  $p < 0.05$  corrected for multiple testing). Hemodynamic correlates linked to IED are detected along the insula and the fusiform gyrus, the superior temporal gyrus and anterior limbic lobe, the anterior cingulate gyrus and contralateral in the insula, superior temporal gyrus, occipital lobe and posterior cingulate gyrus

exhibit a signature that might be characteristic for distinct focal epilepsy syndromes [18]. All patients in our series presented with HC linked to IEDs within the hippocampus corresponding to the surgically proven SOZ in 8/10 patients and presumed SOZ in 2/10 patients based on the concordant semiology, ictal telemetry and unilateral hippocampal lesion. The HC extended into the ipsilateral temporopolar and bilateral laterotemporal neocortex and insula. The hippocampus and ipsilateral insula, temporo-polar neocortex and lateral temporal lobe are strongly functionally interconnected during ictal and interictal states [1, 3, 39] and constitute the medial temporal/limbic network involved into the formation of the affective dimension and oro-alimentary behavior in MTLE seizures [21]. Perfusion increase and functional connectivity during focal seizures with oro-alimentary behavior has been demonstrated in the ipsilateral hippocampus, the insula and the temporal pole with widespread extension along the posterior temporal lobe and cerebellum in patients with MTLE [53]. The interictal analysis in the current study suggests that these areas are similarly functionally connected during seizure-free periods.

**Table 3** Clusters of significant rGMV reductions in patients with MTLE compared to age and sex matched healthy controls ( $p < 0.05$ , corrected)

rGMV reduction		$p$ value corrected (cluster level)	MNI coordinates			Cluster size	$T$ (voxel level)
Description			$x$	$y$	$z$		
Global cluster maximum	Local maxima						
<b>Ipsilateral</b>							
Lingual gyrus		0.004	8	-68	5	2,535	7.30
	Lingual gyrus		8	-68	5		
	Posterior cingulate		15	-63	11		
	Parahippocampal gyrus		15	-53	-1		
Middle temporal gyrus		0.0001	47	6	-38	8,653	7.02
	Middle temporal gyrus		47	6	-38		
	Inferior temporal gyrus		48	-13	-31		
	Uncus		25	0	-40		
Insula		0.025	34	12	-8	1,826	6.54
Anterior lobe cerebellum		0.0001	13	-46	-31	4,826	5.91
	Anterior lobe cerebellum		13	-46	-31		
	Posterior lobe cerebellum		15	-43	-40		
Posterior cingulate		0.048	14	-49	23	1,600	5.67
	Posterior cingulate		14	-49	23		
	Precuneus		23	-60	29		

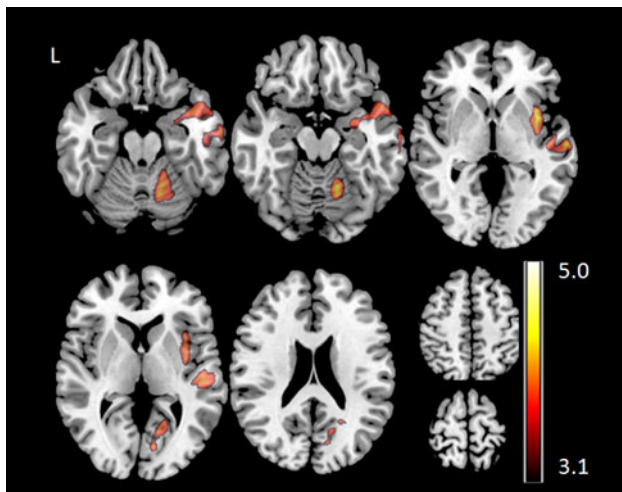


**Fig. 3** Group analysis of the VBM analysis in 10 patients with MTLE ( $t$ -map at  $t > 3.1$  and additional cluster size threshold resulting in  $p < 0.05$  corrected for multiple testing). Abnormalities of relative grey matter volume are detected in the middle temporal gyrus, inferior temporal gyrus and uncus to the hippocampus, the insula, the posterior cingulate and the anterior lobe of the cerebellum

The superior parietal/frontal network incorporates the hippocampus, ipsilateral cingulate cortex and precuneus. Recent literature postulated that posterior midline cortex constitutes the core hub within the default mode network (DMN) of the human brain, with strong connections to the ventral medial prefrontal cortex/anterior cingulate cortex

and inferior lateral parietal [13, 28, 36]. The superior parietal/frontal network is connected with the mesiotemporal structures and involved in memory processing and awareness in the physiological state and may be responsible for impaired consciousness during propagation of epileptic seizures [6, 50, 51]. We found bilaterally distributed HCs in the cingulate cortex and inferior lateral parietal cortex. The involvement of the posterior part of the DMN in MTLE has been consistently reported by previous EEG/fMRI studies [18, 32, 35]. Our study detected activations in bilateral posterior cingulate (-10, -16, 35), which is in contrast to previously reported deactivations. Under physiological conditions the hippocampus and the posterior DMN show positive functional connectivity [28, 51]. In idiopathic generalized epilepsy, positive BOLD correlates in the DMN occurring prior to IEDs and negative BOLD correlates simultaneously to the IEDs are observed, suggesting a role of the DMN in preparation/genesis of epileptic seizures [4]. However, cortical BOLD correlates in idiopathic generalized epilepsies may be positive or negative, potentially representing different underlying pathophysiological traits [9]. In MTLE the different polarity of BOLD correlates in the DMN observed in the different studies may, as well, represent different propagation properties of epileptic activity within an epileptic network of MTLE. The role of the DMN in focal epilepsy remains to be further elucidated.

Among the structurally altered brain areas in temporal lobe epilepsy the occipital lobe, cerebellum and posterior

**Table 4** Overlap of HC and anatomical changes in patients with MTLE

Overlay of hemodynamic correlates and anatomical changes					
Anatomical localization	MNI coordinates of center of gravity			Cluster size	DSC in %
	x	y	z		
Ipsilateral					
Hippocampus	26	−3	−21	29	0.5
Insula/Globus pallidum	37	−4	−6	576	33.1
Inferior temporal gyrus/temporo-polar	46	6	−33	880	14.2
Superior temporal gyrus	52	−6	−8	191	3.1
Cerebellum	20	−50	−16	76	1.4

DSC dice similarity coefficient

temporal lobe are core structures for tasks that require intense information processing abilities [55]. These areas include a physiologically active alertness network that prepares the brain for sensory stimuli and maintains this high level of readiness. Neuronal damage within these regions has been demonstrated to affect physiological network circuits of memory and alertness and may result in deficits of intelligence, memory, and vulnerability to psychiatric disorders in MTLE patients [55]. Increased HCs to IEDs were similarly detected in our study within core structures of the alertness network in the fusiform gyrus and cerebellum and reduced rGMV in the ipsilateral occipital lobe. The same areas, especially the ipsilateral lingual gyrus and cerebellum have been consistently identified to be active during ictal studies [53]. The involved cortices lie along the occipito-temporal connections supplied by inferior longitudinal fasciculus [10], suggesting a direct propagation pathway from the antero-temporal to the occipital lobe.

The structural analysis revealed a pattern of rGMV reduction within the ipsilateral mesial temporal lobe, the insula, anterior temporal and posterior temporal cortices, precuneus and posterior cingulate gyrus. Several studies that investigated the extent of grey matter changes in patients with MTLE have consistently identified grey matter atrophy in the mesial temporal lobe and temporal neocortex [5, 7, 16, 30, 42, 44, 45]. Widespread rGMV reductions along cortical structures that form an ipsilateral medial temporal/limbic network, a medial occipital/lateral temporal network and a superior parietal/medial frontal network functionally connected to the hippocampus have been identified previously [10] along with altered ictal metabolism [28]. The spatial overlap between rGMV reductions and *interictal* functional activations in the limbic structures within the ipsilateral temporal lobe and adjacent neocortical structures provide further evidence that these regions play a role in seizure spread and evolution of mesial temporal lobe seizures [3]. This is in keeping with previous studies that demonstrated that grey matter

alterations in the mesial temporal lobe may influence functional connectivity in remote regions, indicating that “morphology impacts function in MTLE” [52]. The quantitative overlap of functional and structural cluster did not reach similarly high values as reported in methodological papers comparing different analysis techniques on the same data set [11, 31], but is in line with overlay measures between different modalities [34]. In MTLE there is converging clinical and neurophysiological evidence, that functional changes occur beyond the structural modification [17] and cortical abnormalities may influence the metabolic functioning [43]. Both epilepsy specific aspects may contribute to the low DSC values in the present study. Due to the small number of patients enrolled into the study, we could not examine differences between left and right sided MTLEs, and cortical abnormalities in MTLE within the precentral and postcentral neocortex as described in previous work [5] were not detected in our series, presumably due to the small sample size for VBM studies. Future work may integrate individual seizure semiology into the functional and structural network analysis; here, differences would be expected if temporal epilepsy with neocortical SOZ would be included.

In summary, we have demonstrated that HC to IED in MTLE include widespread areas along the medial temporal/limbic network, the medial occipital/lateral temporal network and the superior parietal/medial frontal network. The spatial distribution of functional activity overlaps with cortical abnormalities notably in the medial temporal/limbic network ipsilateral to the SOZ indicating that chronic alterations of brain activity are linked to widespread structural changes. Our data further support the concept of MTLE as a disorder of correlated large-scale functional and structural networks.

**Acknowledgments** We are grateful to M. Fuchs for his support in data collection.

**Conflicts of interest** This project was funded by the Swiss National Science Foundation grants [320000-108321/1], [33CM30-140332]



and [33CM30-124089]. No additional conflict of interest relevant to this article was reported.

## References

1. Alarcon G, Guy CN, Binnie CD, Walker SR, Elwes RD, Polkey CE (1994) Intracerebral propagation of interictal activity in partial epilepsy: implications for source localisation. *J Neurol Neurosurg Psychiatry* 57:435–449
2. Bartolomei F, Chauvel P, Wendling F (2008) Epileptogenicity of brain structures in human temporal lobe epilepsy: a quantified study from intracerebral EEG. *Brain* 131:1818–1830
3. Bartolomei F, Wendling F, Bellanger JJ, Regis J, Chauvel P (2001) Neural networks involving the medial temporal structures in temporal lobe epilepsy. *Clin Neurophysiol* 112:1746–1760
4. Benuzzi F, Mirandola L, Pugnaghi M, Farinelli V, Tassinari CA, Capovilla G, Cantalupo G, Beccaria F, Nichelli P, Meletti S (2012) Increased cortical BOLD signal anticipates generalized spike and wave discharges in adolescents and adults with idiopathic generalized epilepsies. *Epilepsia* 53:622–630
5. Bernhardt BC, Bernasconi N, Concha L, Bernasconi A (2010) Cortical thickness analysis in temporal lobe epilepsy: reproducibility and relation to outcome. *Neurology* 74:1776–1784
6. Blumenfeld H, McNally KA, Vanderhill SD, Paige AL, Chung R, Davis K, Norden AD, Stokking R, Studholme C, Novotny EJ Jr, Zubal IG, Spencer SS (2004) Positive and negative network correlations in temporal lobe epilepsy. *Cereb Cortex* 14:892–902
7. Bonilha L, Edwards JC, Kinsman SL, Morgan PS, Fridriksson J, Rorden C, Rumboldt Z, Roberts DR, Eckert MA, Halford JJ (2010) Extrahippocampal gray matter loss and hippocampal deafferentation in patients with temporal lobe epilepsy. *Epilepsia* 51:519–528
8. Bonilha L, Rorden C, Appenzeller S, Coan AC, Cendes F, Li LM (2006) Gray matter atrophy associated with duration of temporal lobe epilepsy. *Neuroimage* 32:1070–1079
9. Carney PW, Masterton RA, Flanagan D, Berkovic SF, Jackson GD (2012) The frontal lobe in absence epilepsy: EEG-fMRI findings. *Neurology* 78:1157–1165
10. Catani M, Jones DK, Donato R, Ffytche DH (2003) Occipito-temporal connections in the human brain. *Brain* 126:2093–2107
11. Chupin M, Hammers A, Liu RS, Colliot O, Burdett J, Bardinet E, Duncan JS, Garnero L, Lemieux L (2009) Automatic segmentation of the hippocampus and the amygdala driven by hybrid constraints: method and validation. *Neuroimage* 46:749–761
12. Coan AC, Appenzeller S, Bonilha L, Li LM, Cendes F (2009) Seizure frequency and lateralization affect progression of atrophy in temporal lobe epilepsy. *Neurology* 73:834–842
13. Cole DM, Smith SM, Beckmann CF (2010) Advances and pitfalls in the analysis and interpretation of resting-state FMRI data. *Front Syst Neurosci* 4:8
14. Damoiseaux JS, Rombouts SA, Barkhof F, Scheltens P, Stam CJ, Smith SM, Beckmann CF (2006) Consistent resting-state networks across healthy subjects. *Proc Natl Acad Sci USA* 103:13848–13853
15. Delorme A, Makeig S (2004) EEGLAB: an open source toolbox for analysis of single-trial EEG dynamics including independent component analysis. *J Neurosci Methods* 134:9–21
16. Duzel E, Schiltz K, Solbach T, Peschel T, Baldeweg T, Kaufmann J, Szentkuti A, Heinze HJ (2006) Hippocampal atrophy in temporal lobe epilepsy is correlated with limbic systems atrophy. *J Neurol* 253:294–300
17. Engel J Jr, Brown WJ, Kuhl DE, Phelps ME, Mazzotta JC, Crandall PH (1982) Pathological findings underlying focal temporal lobe hypometabolism in partial epilepsy. *Ann Neurol* 12:518–528
18. Fahoum F, Lopes R, Pittau F, Dubeau F, Gotman J (2012) Widespread epileptic networks in focal epilepsies-EEG-fMRI study. *Epilepsia* 53(9):1618–1627
19. Forman SD, Cohen JD, Fitzgerald M, Eddy WF, Mintun MA, Noll DC (1995) Improved assessment of significant activation in functional magnetic resonance imaging (fMRI): use of a cluster-size threshold. *Magn Reson Med* 33:636–647
20. Friston KJ, Stephan KE, Lund TE, Morcom A, Kiebel S (2005) Mixed-effects and fMRI studies. *Neuroimage* 24:244–252
21. Gloor P, Olivier A, Quesney LF, Andermann F, Horowitz S (1982) The role of the limbic system in experiential phenomena of temporal lobe epilepsy. *Ann Neurol* 12:129–144
22. Glover GH (1999) Deconvolution of impulse response in event-related BOLD fMRI. *Neuroimage* 9:416–429
23. Gotman J (2008) Epileptic networks studied with EEG-fMRI. *Epilepsia* 49(Suppl 3):42–51
24. Guye M, Regis J, Tamura M, Wendling F, McGonigal A, Chauvel P, Bartolomei F (2006) The role of corticothalamic coupling in human temporal lobe epilepsy. *Brain* 129:1917–1928
25. Hauf M, Jann K, Schindler K, Scheidegger O, Meyer K, Rummel C, Mariani L, Koenig T, Wiest R (2012) Localizing seizure-onset zones in presurgical evaluation of drug-resistant epilepsy by electroencephalography/fMRI: effectiveness of alternative thresholding strategies. *AJNR Am J Neuroradiol* 33:1818–1824
26. Hesse C, James C (2005) Tracking epileptiform activity in the multichannel ictal EEG using spatially constrained independent component analysis. *Conf Proc IEEE Eng Med Biol Soc* 2:2067–2070
27. Jackson GD, Badawy RA (2011) Selecting patients for epilepsy surgery: identifying a structural lesion. *Epilepsy Behav* 20:182–189
28. Jann K, Kottlow M, Dierks T, Boesch C, Koenig T (2010) Topographic electrophysiological signatures of FMRI resting state networks. *PLoS ONE* 5:e12945
29. Jann K, Wiest R, Hauf M, Meyer K, Boesch C, Mathis J, Schroth G, Dierks T, Koenig T (2008) BOLD correlates of continuously fluctuating epileptic activity isolated by independent component analysis. *Neuroimage* 42:635–648
30. Keller SS, Mackay CE, Barrick TR, Wiesmann UC, Howard MA, Roberts N (2002) Voxel-based morphometric comparison of hippocampal and extrahippocampal abnormalities in patients with left and right hippocampal atrophy. *Neuroimage* 16:23–31
31. Khan AR, Wang L, Beg MF (2008) FreeSurfer-initiated fully-automated subcortical brain segmentation in MRI using large deformation diffeomorphic metric mapping. *Neuroimage* 41:735–746
32. Kobayashi E, Grova C, Tyvaert L, Dubeau F, Gotman J (2009) Structures involved at the time of temporal lobe spikes revealed by interindividual group analysis of EEG/fMRI data. *Epilepsia* 50:2549–2556
33. Krendl R, Lurger S, Baumgartner C (2008) Absolute spike frequency predicts surgical outcome in TLE with unilateral hippocampal atrophy. *Neurology* 71:413–418
34. Larsen S, Kikinis R, Talos IF, Weinstein D, Wells W, Golby A (2007) Quantitative comparison of functional MRI and direct electrocortical stimulation for functional mapping. *Int J Med Robot* 3:262–270
35. Laufs H, Hamandi K, Salek-Haddadi A, Kleinschmidt AK, Duncan JS, Lemieux L (2007) Temporal lobe interictal epileptic discharges affect cerebral activity in “default mode” brain regions. *Hum Brain Mapp* 28:1023–1032
36. Li B, Wang X, Yao S, Hu D, Friston K (2012) Task-dependent modulation of effective connectivity within the default mode network. *Front Psychol* 3:206

37. Luders E, Gaser C, Jancke L, Schlaug G (2004) A voxel-based approach to gray matter asymmetries. *Neuroimage* 22:656–664
38. Luo C, Qiu C, Guo Z, Fang J, Li Q, Lei X, Xia Y, Lai Y, Gong Q, Zhou D, Yao D (2011) Disrupted functional brain connectivity in partial epilepsy: a resting-state fMRI study. *PLoS ONE* 7:e28196
39. Maillard L, Vignal JP, Gavaret M, Guye M, Biraben A, McGonigal A, Chauvel P, Bartolomei F (2004) Semiologic and electrophysiologic correlations in temporal lobe seizure subtypes. *Epilepsia* 45:1590–1599
40. Meisenzahl EM, Koutsouleris N, Gaser C, Bottlender R, Schmitt GJ, McGuire P, Decker P, Burgermeister B, Born C, Reiser M, Moller HJ (2008) Structural brain alterations in subjects at high-risk of psychosis: a voxel-based morphometric study. *Schizophr Res* 102:150–162
41. Moorhead TW, Job DE, Spencer MD, Whalley HC, Johnstone EC, Lawrie SM (2005) Empirical comparison of maximal voxel and non-isotropic adjusted cluster extent results in a voxel-based morphometry study of comorbid learning disability with schizophrenia. *Neuroimage* 28:544–552
42. Mueller SG, Laxer KD, Barakos J, Cheong I, Garcia P, Weiner MW (2009) Widespread neocortical abnormalities in temporal lobe epilepsy with and without mesial sclerosis. *Neuroimage* 46:353–359
43. Oakes TR, Fox AS, Johnstone T, Chung MK, Kalin N, Davidson RJ (2007) Integrating VBM into the general linear model with voxelwise anatomical covariates. *Neuroimage* 34:500–508
44. Pail M, Brazdil M, Marecek R, Mikl M (2010) An optimized voxel-based morphometric study of gray matter changes in patients with left-sided and right-sided mesial temporal lobe epilepsy and hippocampal sclerosis (MTLE/HS). *Epilepsia* 51:511–518
45. Riederer F, Lanzenberger R, Kaya M, Prayer D, Serles W, Baumgartner C (2008) Network atrophy in temporal lobe epilepsy: a voxel-based morphometry study. *Neurology* 71:419–425
46. Santana MT, Jackowski AP, da Silva HH, Caboclo LO, Centeno RS, Bressan RA, Carrete H Jr, Yacubian EM (2010) Auras and clinical features in temporal lobe epilepsy: a new approach on the basis of voxel-based morphometry. *Epilepsy Res* 89:327–338
47. Spencer SS (2002) Neural networks in human epilepsy: evidence of and implications for treatment. *Epilepsia* 43:219–227
48. Sutula TP, Hagen J, Pitkanen A (2003) Do epileptic seizures damage the brain? *Curr Opin Neurol* 16:189–195
49. Tao JX, Chen XJ, Baldwin M, Yung I, Rose S, Frim D, Hawes-Ebersole S, Ebersole JS (2011) Interictal regional delta slowing is an EEG marker of epileptic network in temporal lobe epilepsy. *Epilepsia* 52:467–476
50. Thiebaut de Schotten M, Urbanski M, Duffau H, Volle E, Levy R, Dubois B, Bartolomeo P (2005) Direct evidence for a parietal-frontal pathway subserving spatial awareness in humans. *Science* 309:2226–2228
51. Vincent JL, Snyder AZ, Fox MD, Shannon BJ, Andrews JR, Raichle ME, Buckner RL (2006) Coherent spontaneous activity identifies a hippocampal-parietal memory network. *J Neurophysiol* 96:3517–3531
52. Voets NL, Beckmann CF, Cole DM, Hong S, Bernasconi A, Bernasconi N (2012) Structural substrates for resting network disruption in temporal lobe epilepsy. *Brain* 135(Pt 8):2350–2357
53. Weder BJ, Schindler K, Loher TJ, Wiest R, Wissmeyer M, Ritter P, Lovblad K, Donati F, Missimer J (2006) Brain areas involved in medial temporal lobe seizures: a principal component analysis of ictal SPECT data. *Hum Brain Mapp* 27:520–534
54. Zhang Z, Lu G, Zhong Y, Tan Q, Liao W, Chen Z, Shi J, Liu Y (2009) Impaired perceptual networks in temporal lobe epilepsy revealed by resting fMRI. *J Neurol* 256:1705–1713
55. Zheng J, Qin B, Dang C, Ye W, Chen Z, Yu L (2012) Alertness network in patients with temporal lobe epilepsy: a fMRI study. *Epilepsy Res* 100:67–73